Electrocodeposition of Nickel−Diamond and Cobalt−Chromium Carbide in Low Gravity

Hind Abi-Akar and Clyde Riley*

Department of Chemistry and Materials Science, The University of Alabama in Huntsville, Huntsville Alabama 35899

George Maybee

McDonnell Douglas Aerospace Company, Huntsville, Alabama 35814

Received October 11, 1995. Revised Manuscript Received July 11, 1996[⊗]

Codeposition of particles and metals was studied under low-gravity conditions. Ni−diamond and Co−chromium carbide coatings were investigated. Experiments were run aboard two sounding rockets, each providing 7 min of $10^{-4}g$, and one shuttle mission providing 4 h of deposition. Reduced gravity proved to eliminate sedimentation and edge effects and promote easier particle dispersion in the electrolyte, yielding uniformly distributed particles in the metal matrix. Large nonconducting diamond particles were codeposited in higher volume percents as opposed to bench experiments. The trend was opposite for particles of ≤ 1 μm size with fine chromium carbide particles depositing in higher volume percent in 1*g* than low *g*.

1. Introduction

Electrocodeposition of inert particles with a metal matrix is an important process because of its utility for producing composites.[1−10] Controlled thickness coatings in a variety of metal/particle compositions can be readily prepared by this technique. Electrocodeposited coatings serve diverse engineering applications including improved wear resistance, self-lubrication, and dispersion hardening.[2−5,9,10] Thoma has documented the improvements in hardness relative to neat metals for several electrocodeposited coatings of cobalt, and nickel with cermets as a function of temperature.[9] Uniform distribution and increased percentage of inert particles in the metal matrix were found to be crucial to the enhanced performance of the composite. Dennis et al. have made similar studies on nickel−chromium carbide codeposits that also include wear-resistant data.[10]

Uniformly dispersed particles in the electrodeposition solution allows a continuous flux of particles to the cathode, where they can be adsorbed and eventually trapped within the growing metal matrix. A satisfactory long adsorption time is essential to the successful anchoring of the particles by the depositing metal.[6,7] Earth's gravitational forces interfere with the dispersion and adsorption processes.[1] Codeposition in a reduced gravity environment would eliminate sedimentation. Since electrical attraction between the surface-absorbed charges on the particles and the cathode cannot now be dominated by gravitation force, there should be a lengthened time period particles are held on the cathode and thus improve incorporation in the forming metal matrix. In general, particles up to 5 μm in diameter have been found to codeposit readily in 1*g*. Larger particles are difficult to codeposit due, most probably, to the increase of the mass/charge ratio that hinders their electrophoretic transport to and retention on the cathode. Particle size, and its implication on the volume percent of occluded particles, is one of the parameters that can be investigated in low-gravity experiments.

Access to carrier vehicles that allow for experimentation in low gravity, such as KC-135 planes, commercial rockets, and shuttle flights is now possible. We have carried out experimentation in electrocodeposition in reduced gravity using all these vehicles.[1,8] Our research was directed toward two goals: (a) the study of hydrodynamics of particle dispersion in an electrolytic solution; (b) surface distribution and volume percent of codeposited inert particles in a metal matrix under varying operating conditions.

We initiated our codeposition studies with the observation of particle suspension behavior in an electrolytic solution under the reduced gravity conditions produced on a KC-135 aircraft.[1] These experiments were preliminary for codeposition of composite coatings on suborbital rockets and shuttle orbiter flights. The results proved that suspension and dispersion in low gravity are not as complete as expected. Particle clumping, as opposed to complete dispersion, was observed in the electrolytic solutions (Figure 1). The same phenomenon was not detected in similar bench experiments in earth's environment.

We utilized two systems of metal/particles in our work, Ni−diamond and Co−chromium carbide. Influence of particle size and concentration was investigated,

[⊗] Abstract published in *Advance ACS Abstracts,* September 15, 1996.

(1) Riley, C.; Abi-Akar, H.; Benson, B.; Maybee, G. *J. Spacecraft Rockets* **1990**, *27*, No. 4, 386.
(2) Kedward, K. C.; Addisson, C. A.; Tennett, A. A. B. *Trans. Inst. Met. Finishing* **1976**, *54*, 8.
(3) Tomaszewski, T. W.; Tomaszewski, L. C.; Brown, H. *Plating* **1969**, *56*, 1234.
(4) Sato, A.; Suzuki, K. *Met. Finishing* **1984**, *82*, 21.
(5) Vest, E. C.; Bazzarre, D. F. *Met. Finishing* **1967**, *65*, 52.
(6) Guglielmi, N. *J. Electrochem. Soc.* **1972**, *119*, 1009.
(7) Celis, J. P.; Roos, J. R.; Buelens, C. *J. Electrochem. Soc.* **1987**, *134*, 1402.
(8) Abi-Akar, H.; Riley, C.; Maybee, G. *J. Mater. Sci.* **1996**, *31*, 1767.
(9) Thoma, M. *Plating Surf. Finishing* **1984**, *71*, No. 9, 51.
(10) Dennis, J. K.; Sheikh, S. T.; Silverstone, E. C. *Trans. Inst. Met. Finishing* **1981**, *59*, 118.

S0897-4756(95)00483-2 CCC: $12.00

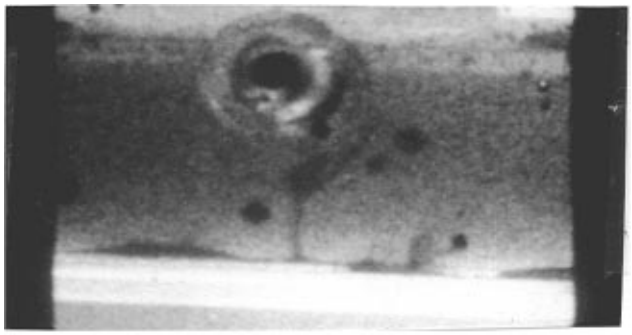

Figure 1. Photograph showing clumping of chromium carbide in electrocodeposition cell in low *g* produced on a KC-135 aircraft.

as well as other parameters such as solution concentration, stirring, and current density. Photography accompanied all codeposition experiments in order to record the movement of particles in the solutions. Rocket flights and Shuttle orbiter flights presented extended periods of uninterrupted low gravity (430 s and up to 72 h, respectively) which allows the resolution of the questions resulting from the KC-135 experiments and the exploration of the codeposition process.

2. Experimental Section

2.1. Experimental Hardware. Ni−diamond and Co−chromium carbide were electrocodeposited under gravity conditions of the order of $10^{-4}-10^{-6}g$ for about 7 min on two sounding rockets (Consorts I and III) and 4 h on GAS-105 aboard the shuttle. These flights were two of a series of five sounding rockets designated Consort's I−V launched at White Sands between 1989 and 1992. All were supported through the University of Alabama in Huntsville's Consortium for Materials Development in Space. The shuttle experiment, designated GAS 105 was a self-contained "gas can" experimental cannister flown in the shuttle bay during June of 1991. Electrocodeposition was performed on each flight in compact specially designed plexiglass cells. The cells were relatively small (6.5 × 2.5 × 2.5 cm), had an electrolyte volume of about 7 mL, could be assembled and disassembled quickly, and were lightweight (Figure 2). They were subjected to −15 °C freeze tests without bursting and could be over pressurized about 1 atm before any leakage occurred. Since photography accompanied the deposition process, the cell walls facing the camera were buffed until optically clear so the cell contents could be photographed. Small motors rotating stirring bars were utilized to agitate the cell contents and suspend the particles. These motors were positioned perpendicular to the cell body and opposite optical viewing faces of the cells. While some were mounted as a cell-motor couple (GAS 105 experiment), usually the cells and motors were mounted separately. Stirring, stirring bar coupling, ease of mounting, design simplicity, particle suspension, and vibration noise were considered in choosing the stirring motors. Low vibrational noise output was critical in maintaining the payload *g* level in the rockets at less than $10^{-4}g$. Gear motors, to which round horseshoe magnets were mounted, were initially used in the low-*g* experiments. In subsequent experiments 1212 MicroMo motors gave better compliance with the requirements, especially the low noise level, and were consequently employed. Modified $^1/_2$ in. × $^1/_8$ in. stirring bars were utilized. Glass covering with two circular ridges on the stirring bars replaced the conventional Teflon coating. The ridges served as spacers to reduce the magnetic attraction of the bars to the magnetic Ni or Co anodes allowing them to preferentially couple to the rotating polar magnets.

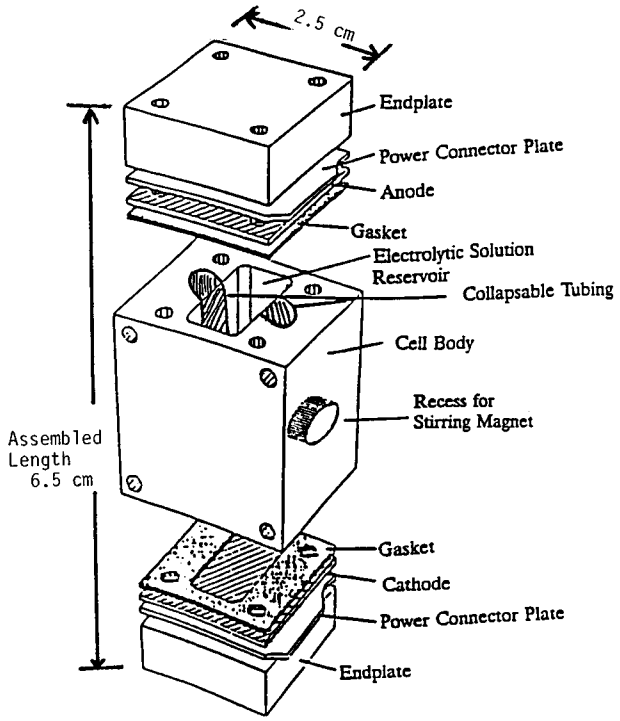

Figure 2. Schematic of electrocodeposition cells.

Cells were sealed free of gas bubbles after filling with electrolytic solutions that included

Ni Electrolytes		I	II
nickel sulfamate	$(H_2NSO_3)Ni{\cdot}4H_2O$	600 g/L	450 g/L
nickel chloride	$NiCl_2{\cdot}6H_2O$	25 g/L	15 g/L
boric acid	H_3BO_3	30 g/L	37 g/L
		pH 3.5−4.0	pH 2.5−3.0
		Ni anode	Ni anode

Solution 1: electrolyte I + 18 g/L 35−45 μm diamond particles
Solution 2: electrolyte II + 35 g/L 35−45 μm diamond particles
Solution 3: electrolyte II + 35 g/L 5 μm diamond particles
Solution 4: electrolyte II + 35 g/L ≤1 μm diamond particles

Co Electrolytes		III	IV
cobalt sulfate	$CoSO_4{\cdot}7H_2O$	500 g/L	450 g/L
sodium chloride	NaCl	17 g/L	17 g/L
boric acid	H_3BO_3	20−35 g/L	30 g/L
		pH 4.0−5.0	pH 4.0−5.0
		Co anode	Co anode

Solution 5: electrolyte III + 35 g/L 1−10 μm Cr_3C_2 particles
Solution 6: electrolyte IV + 300−350 g/L 1−10 μm Cr_3C_2 particles
Solution 7: electrolyte IV + 300−350 g/L ≤1 μm Cr_3C_2 particles

All electrolytes were 0.2 μm filtered, deoxygenated by a N_2 purge for 20 min and degassed under vacuum. Particles were introduced into the cells followed by addition of the electrolytic solutions and sealed bubble free. Typically, the sealed cells were attached to the system base plate 36 h before the rocket flights, up to 3 months preceding the shuttle flight but were prepared only hours before KC-135 flights and placed in position minutes before deposition. These waiting periods were dictated by the logistics of the flights.

Cathode materials were chosen to be inert to eliminate any reaction with the solution during the period that follows experiment integration. Gold-electroplated Cu plates were the materials of choice. The Cu plate was polished to a 0.5 μm finish before depositing at least 5 μm of gold. Anodes, either

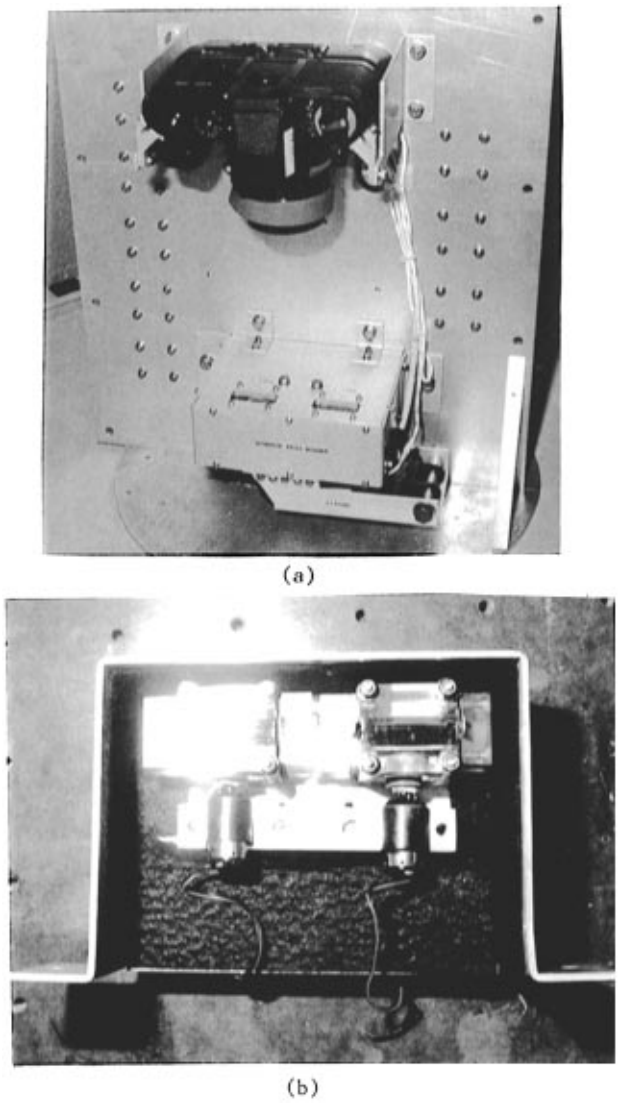

Figure 3. Consort I experimental plate: (a) codeposition face. (b) cells and stirring motors inside the box. Eight electrodeposition cells and controlling electronics on opposite face.

pure Ni or Co, were pickled in suitable acid mixtures and ultrasonically cleaned in high-resistivity DI water. No influencing passivation of anodes or cathodes prepared in this manner was noted in cells stored for up to 3 months prior to operation. Low-gravity electrodeposition cells were run potentiostatically. Galvanostatic operation was found to be unsatisfactory in low *g*. Cells and supporting electronics were mounted on 0.25 in. thick aluminum base plates which were in turn bolted to longeron supports provided for the experiment integration. Space and shape considerations allocated to the GAS can required a hardware design completely different from that of the rocket flights. Figures 3 and 4 are examples of experimental packages utilized in the low-gravity experiments. Each experiment had to pass safety requirements that included vibration, spin, leakage, and freeze tests. There were size, weight, power, and gravity noise restrictions imposed. Safety documentation was also required for each flight.

Several models of Nikon cameras were employed in different flights for photography. F2, F3, and N8008 35 mm models were used. The last model produced the lowest level of vibration during operation. Cameras were attached to the plates with custom-made holders. Indirect strobe lighting was utilized.

Dedicated electronic systems controlled camera function and cell voltage input and recorded current output of the flight electrocodeposition processes. The degree of electronic control dictated the sophistication level. Our systems evolved from primitive off−on toggles used on KC-135 flights to an electronic

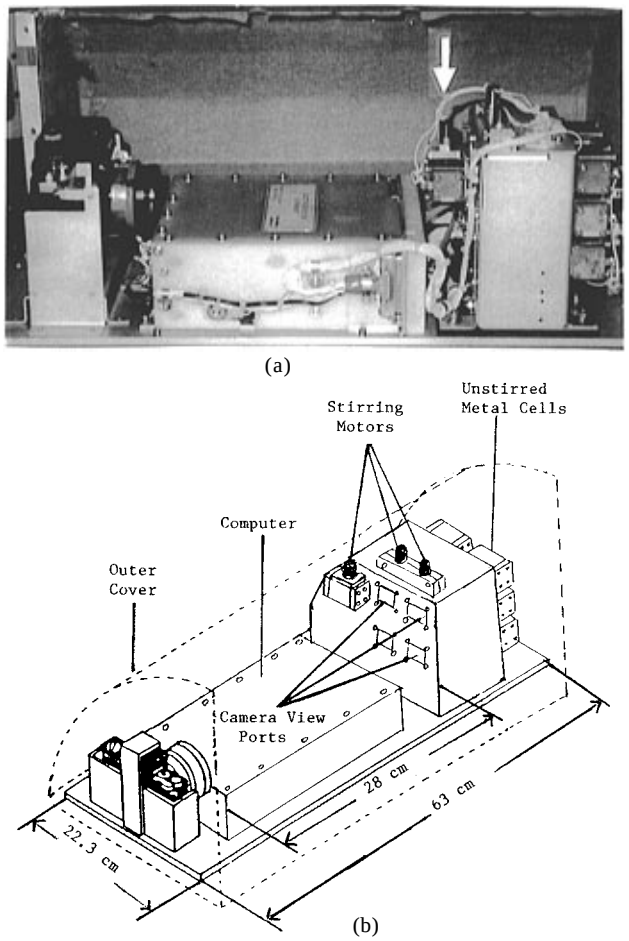

Figure 4. (a) Photograph of experimental shuttle apparatus. Camera and mount (left), computer (center), and cell mounting. Cell and stirring motor combination at the arrow. (b) Schematic of the apparatus showing dimensions and arrangment.

Table 1. Low-Gravity Codeposition Parameters[a]

flight	cell	deposit	V or mA/Cm^2	solution
Consort I	1	Co + Cr_{3C2}[c]	1.5 V	5
	2	Ni + 45 μm D	1.5 V	1
Consort III	1	Ni + 45 μm D	4.5 V	1
	2	Co + Cr_{3C2}[c]	3.0 V	5
	3	Ni + 45 μm D	4.5 V	1
	4	Co + Cr_{3C2}[c]	3.0 V	5
GAS-105	1	Co + Cr_{3C2}[c]	10.0 mA/Cm^2	6
	2	Ni + 5 μm D	10.0 mA/Cm^2	3
	3	Co + Cr_{3C2}[f]	10.0 mA/Cm^2	7
	4	Ni + 45 μm D	10.0 mA/Cm^2	2
	5	Ni + ≤1 μm D	10.0 mA/Cm^2	4

[a] c: coarse, 1−10 μm. f: fine, ≤1 μm. D: diamond.

board with cell voltage regulators, cell current sensing circuits, motor driver circuits, and provisions for charging the flash and timed shutter activation of the camera. Temperature was not controlled but was recorded at 1 s intervals with the aid of a thermistor for the Consort flights. Typically it varied between 21 and 24 °C during the actual electrodeposition and reached as high as 32 °C during reentry. Further sophistication was introduced to the GAS experiment by using a dedicated 12-bit memory computer with three interface electronic boards to control functions. 1*g* reference cells were prepared similarly and run on the bench using the same experimental hardware.

2.2. Process Parameters and Analytical Methods. Table 1 lists the operating parameters and cell contents for the three separate flights. In rocket flights, cells were stirred for 15 s at the onset of low *g*, damped for 10 s, and electrocodeposited for the remaining time (∼400 s). Photographs were taken before and after stirring and at 12 s intervals thereafter. The cells were stirred for the entire shuttle flight,

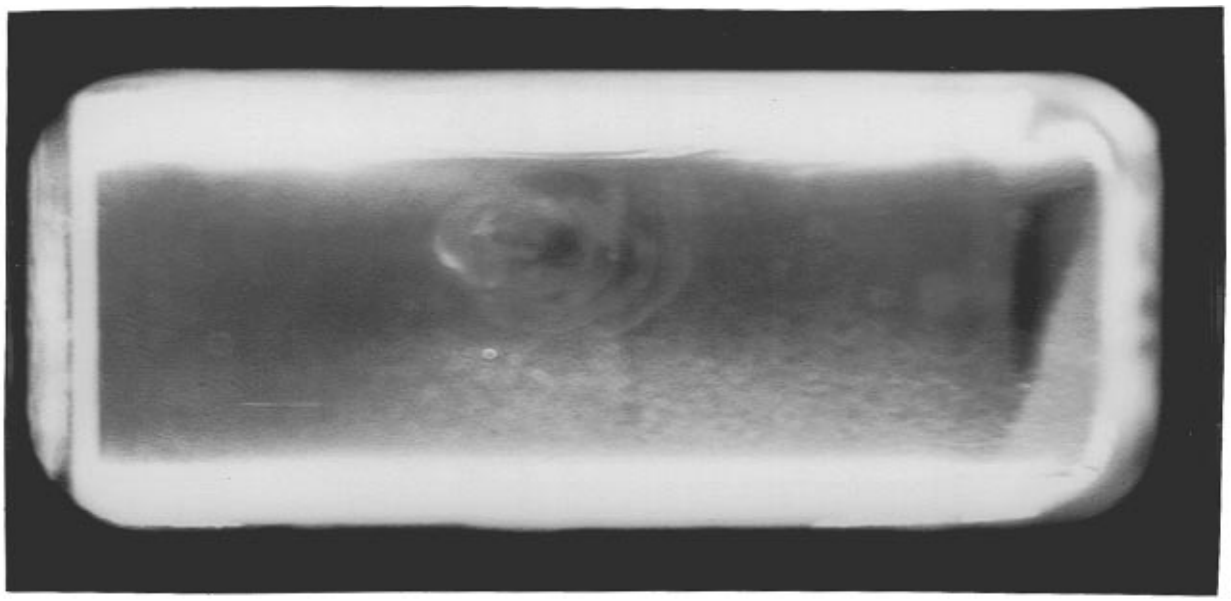

Figure 5. Photograph of cobalt−chromium carbide electrocodeposition cell in flight on Consort I rocket.

but only four cells were photographed throughout the 4 h of codeposition. The first photograph was taken 70 s after codeposition was initiated and successive pictures were taken at 240 s intervals.

Metal deposit thickness was determined by profilometry. SEM micrographs were used for image analysis to evaluate surface particle distribution and content for the samples from the rocket flights where deposited metal matrixes were only 5−7 μm thick and did not fully encapsulate the particle. However, for the shuttle-prepared samples, the composite depositions were prepared over a 4 h period, and thus the particulates may be completely encapsulated (coatings 45−175 μm thick) making them invisible to the SEM. Hence, particle content evaluation required a combination of image and gravimetric analysis. Subsequent to image analysis, part of the deposit was stripped and the dissolute chemically analyzed for its metal concentration. Cross sectional imaging while valuable for a 3-dimensional distribution determination requires destructive sample preparation and would have degraded the gravimetric analysis of our limited number of samples.

2.3. Gravimetric and Chemical Analysis. Ni−diamond and Co−chromium carbide codeposites obtained on the shuttle experiment were gravimetrically and chemically analyzed according to the following steps:

(i) Part of the deposit was dissolved anodically in a 12.5 mL/L of HCl solution at a rate of 10−20 mA/cm^2.[11]

(ii) The deposit was weighed before and after dissolution in order to determine the total content of metal and particles.

(iii) The solution resulting from the dissolution was filtered and weighed for particle mass.

(iv) Metal ion concentration in the filtrate was determined spectrophotometrically after suitable complexing to enhance their absorption.

Cobalt ion concentration was determined using a thiocyanate complex as outlined by Pyatnistskii.[12] Since chromium carbide was now freed from the cobalt matrix and exposed to the dissolution medium, it was essential to verify that these cermets are not affected because their dissolution could interfere in the complexing and analysis process. The solubility of chromium carbide in the HCl solution was tested and found to be negligible, and the Cr−thiocyanate complex was found to absorb at a different wavelength than the Co−thiocyanate complex. Therefore, no interference of chromium carbide in the process is expected.

Ni ions were complexed with oximes following Pershkova and Sarostina.[13] NH_4OH was added to Ni solution, followed by addition of dimethylglyoxime in ethyl alcohol. The resulting Ni complex precipitate was then extracted by chloroform and its optical density determined.

3. Results

3.1. Rocket Flights. Flight photographs showed the diamond and chromium carbide particles were suspended but tended to accumulate around the sides of the cell cavities for our experimental system. Figure 5 shows a photograph of Cr_3C_2 in cobalt on the Consort I rocket. The stirring bar has coupled to the magnet and is suspending the carbide. However, the lower right-hand corner shows an accumulation of Cr_3C_2.

Nickel−diamond: SEM micrographs of the codeposited surfaces from the two rocket flights showed the incorporation of small particles of the order 10 μm or less even though the average size for the particle distribution particle was 45 μm (Figure 6a). The short duration of the deposition did not allow adequate time for the Ni matrix to become thick enough to secure larger particles. Identical crevices were distributed uniformly over the deposited surface (Figure 6b). We attributed these "tracks" to the larger diamond particles which, after being adsorbed on the surface, detached, leaving behind these temporarily protected sites. 1*g* counterpart preparations with the same cells exhibited a negligible incorporation rate of any diamond particles associated with this size distribution.

Cobalt−chromium carbide: Uniform distribution of clusters of chromium carbide particles on the cobalt deposit was observed (Figure 7). It is noted that cobalt nucleates on the chromium carbide clusters due to the conducting nature of the particles. Edge effects, produced by our cell configuration, prevalent in the 1*g* counterparts due to particle sedimentation were not noticeable in the low-*g* prepared surfaces. Conglomerates of chromium carbide particles were also observed.

3.2. Shuttle Experiment. *3.2.1. Photographic Data Gathering.* Four of the five codeposition cells were

(11) *Metal Finishing*, 48th Guidebook-Directory issue, 1980; Vol. 78, No. 1.

(12) Pyatnitskii, I. V. *Analytical Chemistry of Cobalt*; Ann Arbor-Huprey Science Publishers: Woburn, MA, 1969.

(13) Peshkova, V. M.; Sarostina, V. M. *Analytical Chemistry of Nickel*; Ann Arbor-Huprey Science Publishers: Woburn, MA, 1969.

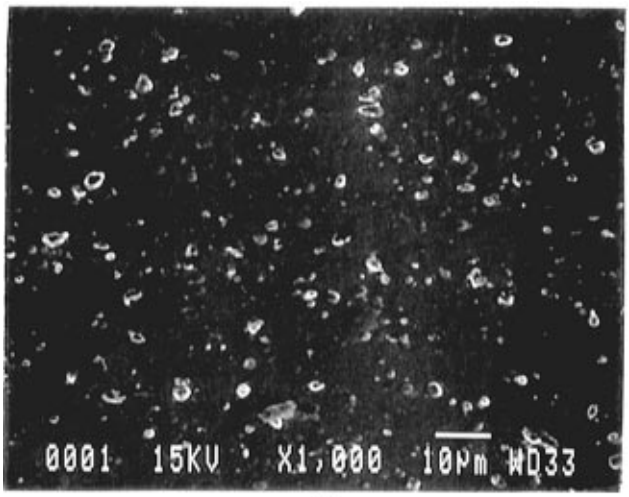

(a)

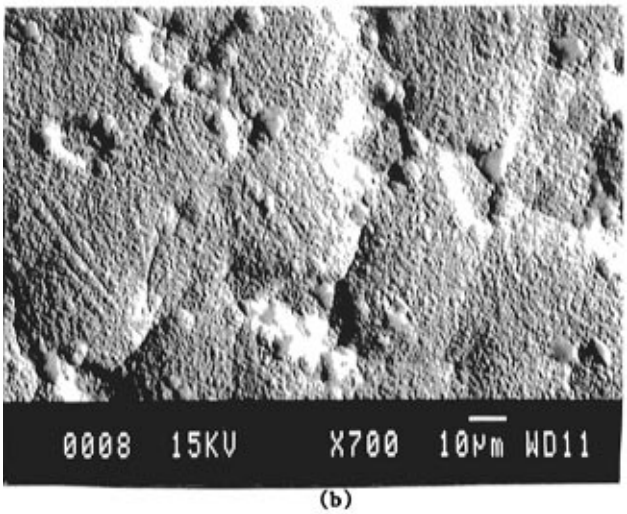

(b)

Figure 6. Consort I, (a) low-*g* Ni−diamond surface; (b) "tracks" of detached diamond particles.

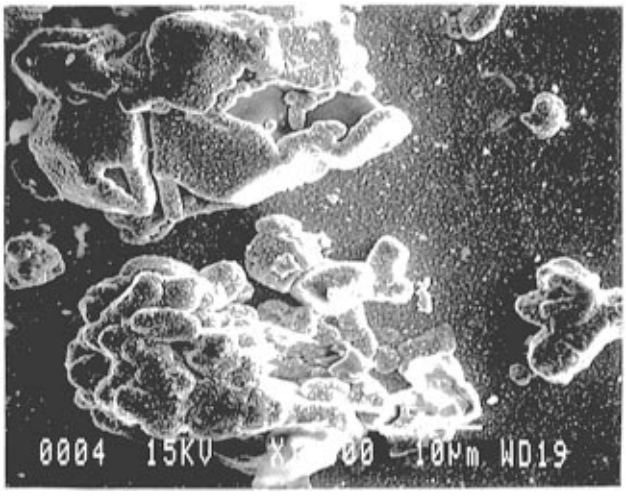

Figure 7. Consort I: cluster of Co−chromium carbide.

photographed throughout the 4 h of codeposition. Although ground-based photographs taken with the same camera and flash settings showed the codeposition cells clearly, flight photographs were compromised. The latter photos exhibited green tinge, faded color, and distinct granularity. Furthermore, the negative had an unusual black color. The film was uniformly fogged. All other experiments, utilizing photography and sharing the experimental capsule with us, had similar difficulties with their film, despite the fact they were of different type or manufacturer. Regardless of the poor photo quality, some information could be obtained from the film. Stirring did occur as indicated by particle movement in the cells and stirring bar positional change.

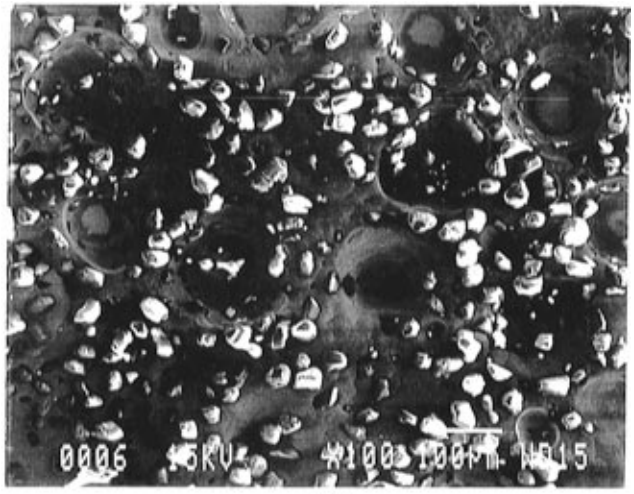

(a)

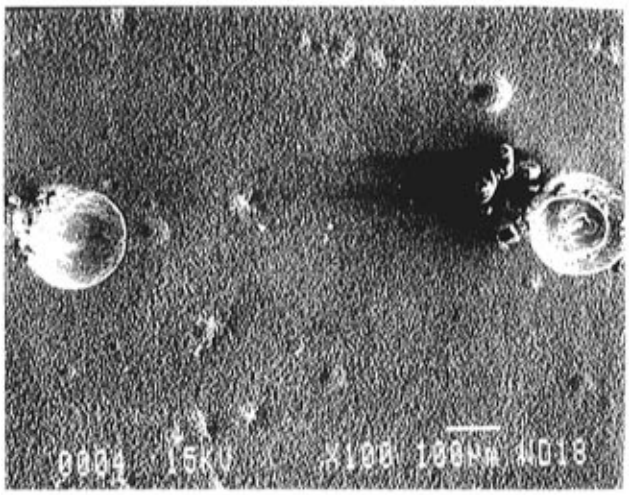

(b)

Figure 8. Shuttle experiment: (a) low *g* Ni + 45 μm diamond; (b) 1*g* control.

3.2.2. Surface Particle Content of the Deposits. SEM micrographs of the surfaces indicated that, unlike preceding rocket flights, the extended period of shuttle produced codeposition resulted in thick deposits with good particle inclusion.

Ni + 45 μm Diamond Particles. Electron microscopy revealed astounding differences between low-*g* and 1*g* codeposits (Figure 8). Image analysis of edge and center locations of the low-*g* sample revealed good coverage of uniformly distributed surface particles and no edge effects. In the 1*g* counterpart, diamond particles were codeposited on one edge only, the edge favored by particle sedimentation due to the cell configuration during operation (Figure 9). Insignificant particle incorporation was obtained in 1*g* regardless of the cell configuration, stirring speed, electrolyte composition or current density. The large pocklike craters evident in Figure 8 are due to the effects of gasing.

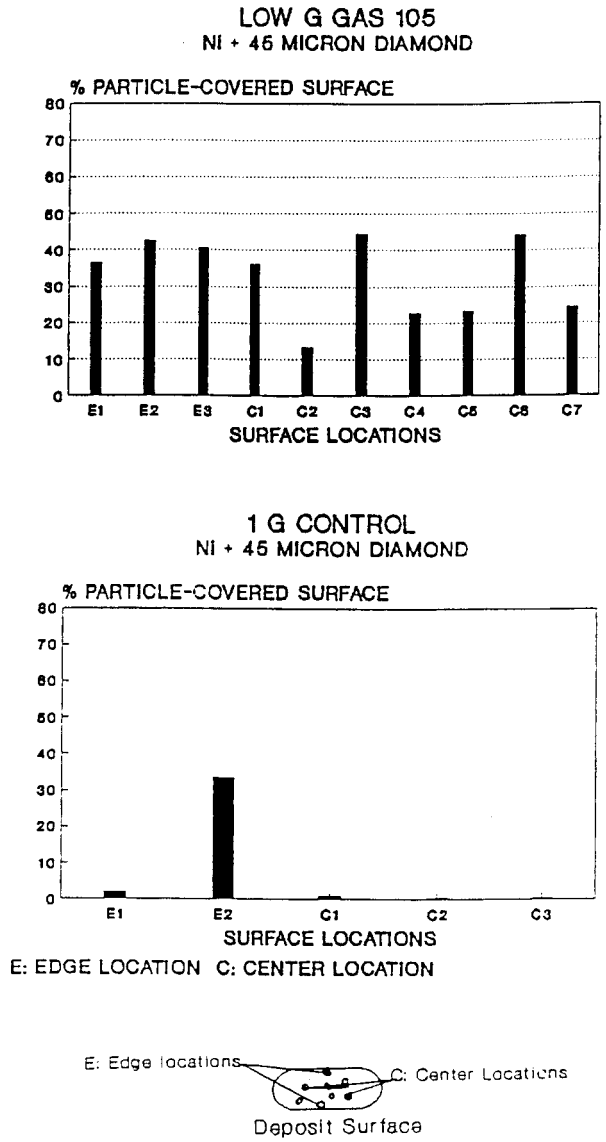

Figure 9. GAS 105, percent surface covered by 45 μm diamond at various locations.

Ni + 5 μm Diamond Particles. Substantial differences in roughness and morphology determind roughness were noted between low-*g* and 1*g* samples (Figure 10). The GAS 105 sample had a profilometry determined roughness of 25 μm with diamond particles occupying "trenches" in the Ni surface. The codepositing nonconductive diamond inhibited the growth of Ni at the codeposition sites, allocating areas around the particles for Ni deposition. The bench control had the particles on top of the surface, instead of more within the surface, with a profilometry determined roughness of 1 μm for the background Ni. Surface coverage represented by bar graphs of Figure 11 was moderately better for the low-*g* produced sample as indicated by a standard deviation $\pm$9.0 versus $\pm$16.5 for the 1*g*. The flight specimen showed an impressive uniformity (including edges), while the lab sample exhibited serious edge effects and lack of uniformity.

Ni + $\leq$1 μm Diamond Particles. Different surface morphologies were obtained for the flight sample and its 1*g* counterpart (Figure 12). While particles were very obvious on the latter, the former is very smooth and bright with few surface particles. Irregular small crevices are noted on the low-*g* prepared surface due to

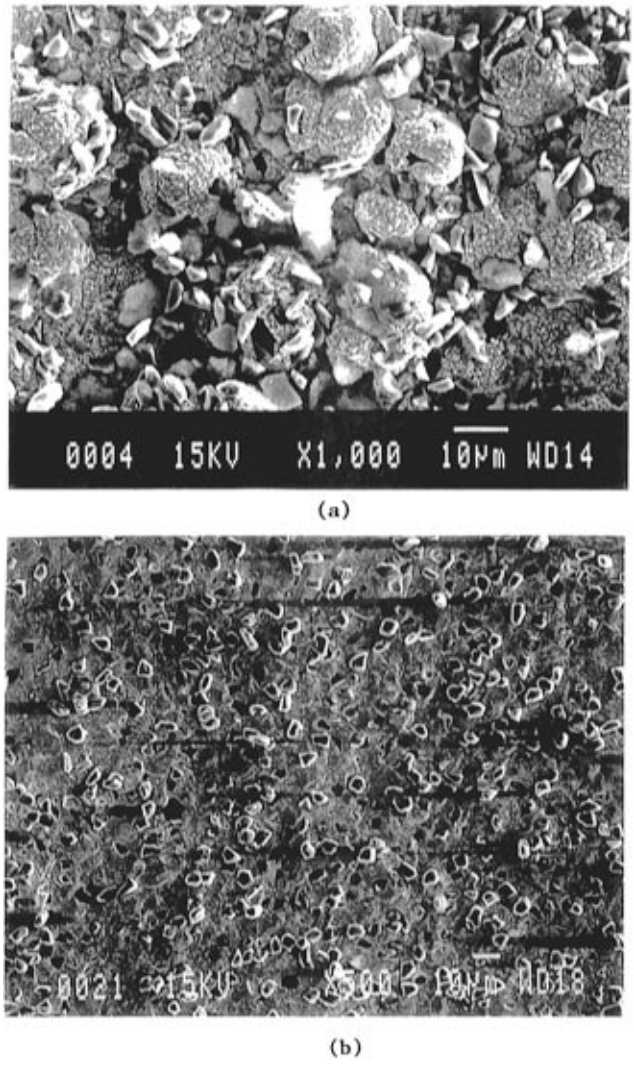

Figure 10. Shuttle experiment: (a) low-*g* Ni + 5 μm diamond; (b) 1*g* control.

nonconducting diamond particles codeposited underneath the surface as verified by the gravimetric determination (Table 2). The output of image analysis (Figure 13) revealed that, unlike the previous samples, for larger particles, a greater number of particles populated the top of the deposit of the terrestrial produced sample than that formed in low *g*. While edge effects are high in the 1*g* sample, homogeneity is good away from the edges.

Co + Coarse Cr_3C_2. The low-*g* sample exhibited uniformly distributed clusters of Co-coated particles (Cr_3C_2 is darker) with increasing roughness at the edges (Figure 14a). Extensive Co nucleation on the particles is apparent (Figure 14b).

Co + Fine Cr_3C_2. In comparison to the coarse codeposition the surface is smoother, even though the percentage of particles incorporated seems to be higher (Figure 15a). We attributed this to less nucleation of Co on the smaller particles. Furthermore, crystallinity of the Co matrix is suppressed. Two 1*g* samples were prepared to be compared to the flight sample. One of the counterparts (labeled stored) was prepared and then stored for the same period of time as the flight sample, while the other (labeled fresh) was prepared and deposited immediately (Figure 15b,c). The former peeled from the surface, was hard and brittle, and possessed

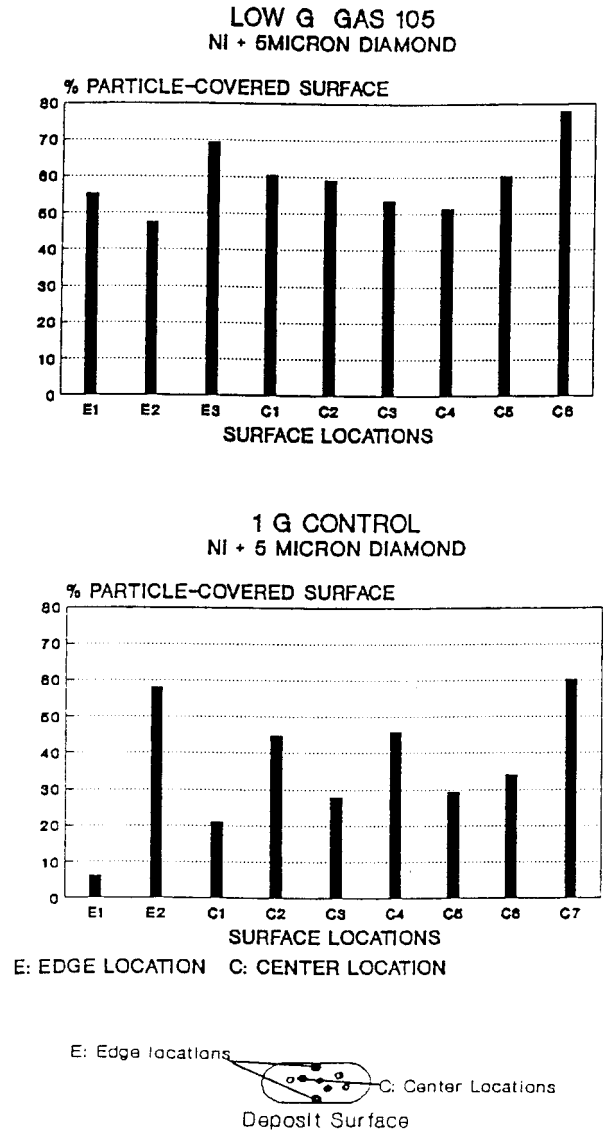

Figure 11. GAS 105, percent surface covered by 5 μm diamond at various locations.

more crystalline formations than the flight sample. The center of this sample did not indicate the presence of any Cr_3C_2, which was later confirmed with energy-dispersive spectroscopy. The metal deposit had a severe edge effect. The surface prepared from a freshly prepared cell was populated with surface particles, its crystalline features were suppressed and it showed edge effects when viewed optically. Although no statistical analysis was performed on the surface, the volume percent of particles was twice that of the stored.

3.2.3. Volume Particle Content of the Deposits. Percentage of particles on the deposit surface is important since it is the interface between the composite film and the outside environment. However, sample characteristics are also dependent upon volume composition. Particle volume contents for the codeposits are presented in Table 2.

Several marked differences appear when comparing codeposition in low *g* and 1*g*. The flight Co + fine chromium carbide deposit contained 3 times the particle weight of the stored sample, and the fresh sample contained double that weight. Unfortunately, we did not have a 1*g* sample for the coarse chromium carbide particles due to unavailability of these particles from

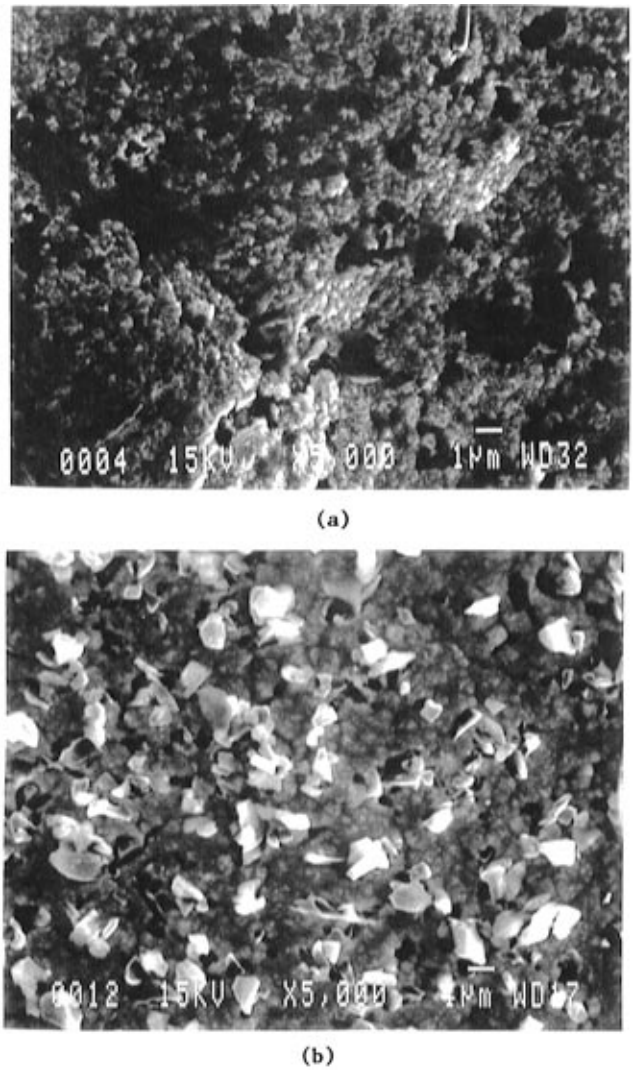

Figure 12. Shuttle experiment: (a) low-*g* Ni + ≤1 μm diamond; (b) 1*g* control.

the original source. The Ni + diamond system with three different size groups offered more chance for contrasting low-*g* and 1*g* codeposition. For nonconducting diamond in Ni, the 1*g* sample particle content increased as the particle size decreased. The 45 μm particle codeposition in low *g* contained over 2.5 times the volume percent of particles deposited in 1*g*, about equal volume percent for the 5 μm particles and only about one-fifth that found in the 1*g* for the smallest diamond particle group.

4. Discussion

Early KC-135 experiments showed that a low-*g* environment can promote anomalities in the suspended particles behavior. Evidence of particle coagulation demonstrated that lack of a dominating gravitational force allowed weaker attractive forces among the particles to be observed.[1] Stirring in low *g* leads to suspension of particles, but total dispersion is not necessarily complete.

Snaith and Groves have noted that a spherical particle may be considered to be keyed into position when the depositing metal matrix has a thickness

Table 2. Percentage of Particles in the Codeposited Surfaces for GAS-105[a]

deposit	environment	wt % particles	wt % metal	vol % particles	deposit thickness (μm)
Co + Cr_3C_2[f]	low *g*	28.1 ± 2.1	71.9 ± 5.5	4.2 ± 0.3	68 ± 1
	1*g* stored	9.4 ± 1.0	90.6 ± 9.3	1.4 ± 0.04	
	1*g* fresh	18.8 ± 0.3	81.2 ± 1.5	2.8 ± 0.05	89 ± 1.5
Co + Cr_3C_2[c]	low *g*	22.2 ± 0.6	77.8 ± 2.1	3.3 ± 0.1	80 ± 1
Ni + 45 μm D	low *g*	66.7 ± 12.8	33.3 ± 6.4	19.0 ± 3.6	120 ± 2
	1*g*	17.3 ± 2.2	82.7 ± 10.6	4.9 ± 0.6	63 ± 1
Ni + 5 μm D	low *g*	39.2 ± 3.0	60.0 ± 5.5	11.12 ± 1.0	175 ± 2
	1*g*	37.0 ± 4.4	63.0 ± 7.5	10.5 ± 1.6	77 ± 1
Ni + ≤1 μm D	low *g*	9.7 ± 0.4	90.3 ± 3.4	2.0 ± 0.1	45 ± 1
	1*g*	46.2 ± 3.2	53.8 ± 3.0	13.2 ± 0.9	65 ± 1

[a] D: diamond particles. f: fine. c: coarse. fresh: the electrolyte was prepared and deposited immediately; stored: the electrolyte had been stored for 3 months to simulate conditions for the low-*g* sample.

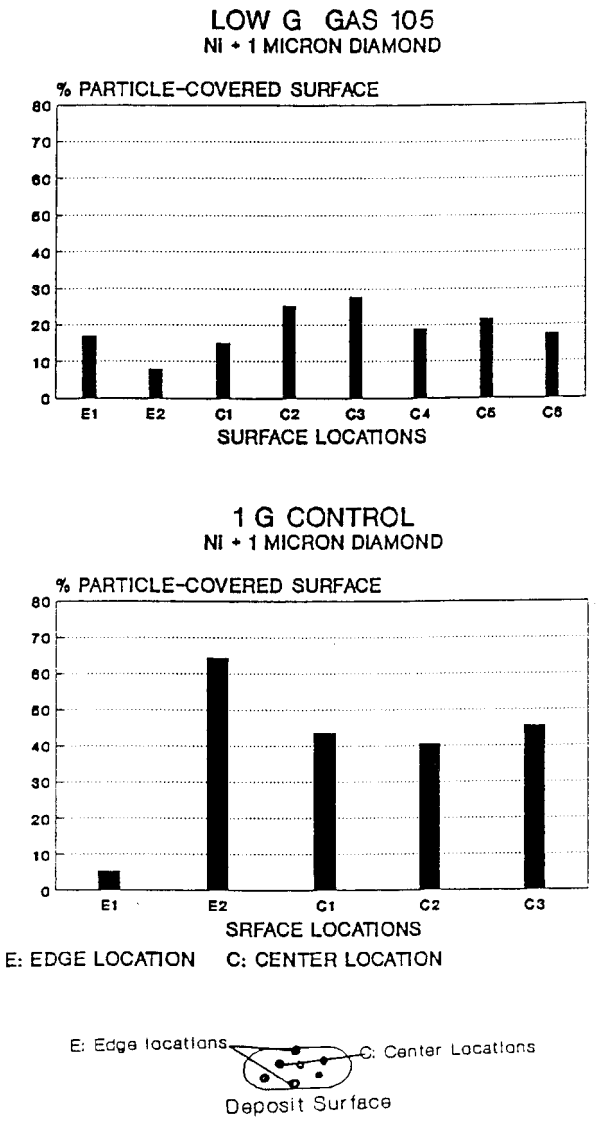

Figure 13. GAS 105, percent surface covered by ≤1 μm diamond at various locations.

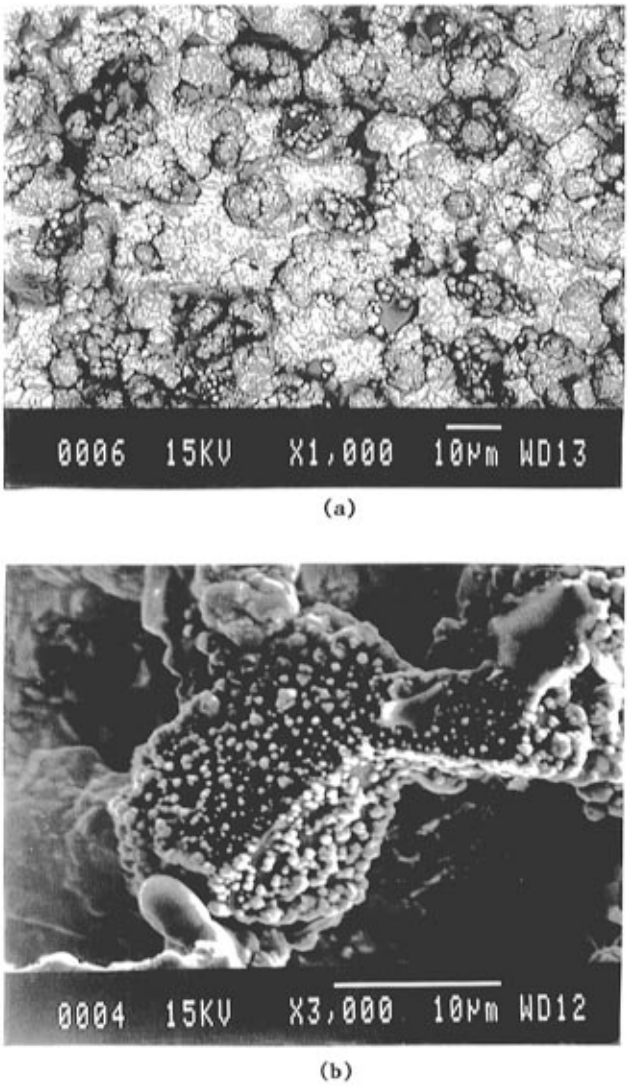

Figure 14. Shuttle experiment: (a) Co + coarse Cr_3C_2; (b) Co nucleating on Cr_3C_2 particle.

greater than half its diameter.[14] Furthermore, a particle must remain stationary and in contact with the cathode surface for the time required to deposit this thickness of metal. This could provide an interpretation of the Consort's Ni−diamond results, where only small particles (10 μm or less) were incorporated. The short deposition time (7 min) and the low current densities (35−42 mA cm^{-2}) allowed only small particles to be keyed into the metal matrix. The tracks apparent in Figure 6b were strong evidence that larger particles did not have enough time to be incorporated.

Initial loose adsorption of particles on the cathode surface could play an important role in the differences noted in low-*g* and 1*g* codeposition. Two different mathematical models aimed at unveiling the mechanism of particle deposition proposed by Gugleilmi and Celis et al., recognized the importance of the adsorption of the particles on the cathode.[6,7] The lack of gravitational force should allow particles to remain loosely attached to the cathode for longer periods before becom-

(14) Snaith, D. W.; Groves, P. D. *Trans. Inst. Met. Finishing* **1972**, *50*, 95.

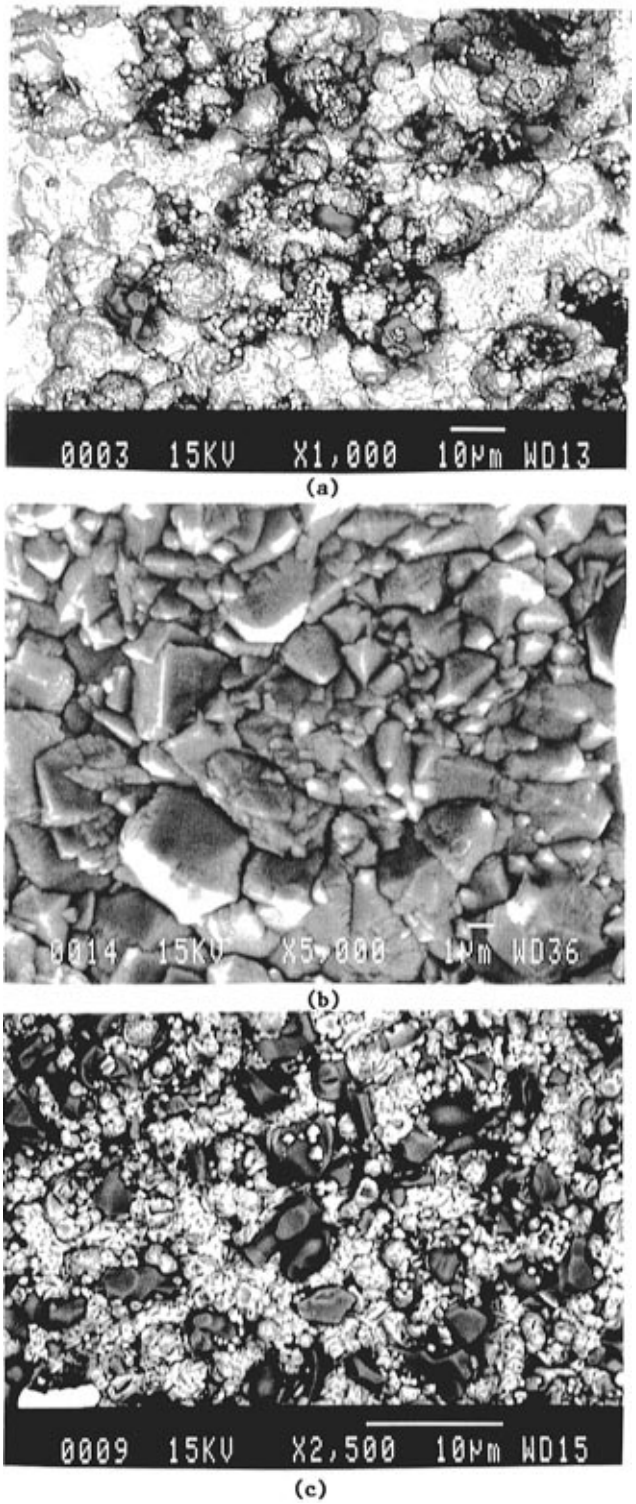

Figure 15. Shuttle experiment: (a) low-*g* Co + fine Cr_3C_2; (b) stored 1*g* control; (c) fresh 1*g* control.

ing detached by hydrodynamic motion, thus creating more favorable conditions for incorporation into the forming metal matrix. This factor is more critical for larger size particles which tend to fall rapidly from the cathode surface in earth-based experiments and would be the cause of the higher volume percent of 45 μm diamond particles obtained in low *g* compared to the Earth-based sample.

The stirring mechanism utilized in our systems was dictated by simplicity, limited experiment size, acceptable vibration levels, torque, and drag limitations of the motors. Some sort of air-agitation system would have been best, but it could not be accommodated in low *g*. Care was taken to operate the small motors within these limitations and at the same time allow appropriate stirring. Generally, appropriate stirring (100−200 rpm) produces uniform dispersion of particles in the electrolyte, which leads to uniform distribution in the deposit, by providing an adequate supply of particles to the cathode vicinity. The amount of agitation is critical to the particle/cathode collision frequency. A high frequency would sweep the particles away from the cathode and reduce the number of loosely adsorbed particles on the substrate and the time they remain loosely attached.[3,15] This decreases the time for the forming metal matrix to fix the particles. A study of Ni−diamond, Co−chromium carbide, and Co−silicon carbide systems showed that smaller size particles are not as sensitive to agitation.[3,16] This is reflected by the comparable volume percents obtained with 5 μm diamond in low-*g* and 1*g* deposits.

Particle concentration in the electrolyte directly affects its volume percent in the deposit. In general, the greater the concentration, the greater the volume percent, but limits exist. It has been found that very high concentrations in the electrolyte increase geometrical effects and collisions among the moving particles, thus reducing the volume percent in the deposit.[17] Chromium carbide particulates were found to be more prone to this behavior than diamond. The concentrations adopted in our systems were proven by several researchers as well as by bench experiments to provide optimum results.[2,15,17]

The effects of the different codeposition mechanisms of diamond and chromium carbide were apparent throughout our experiments, mainly due to the nonconductive nature of diamond versus the conductive chromium carbide. Electrostatic attraction to the cathode is enhanced for the latter, where it is enveloped in a shorter time than nonconductive diamond. Cathode-attracted conductive chromium carbide can then behave as a deposition site. This can lead to cluster formation as depicted schematically in Figure 16a, which is prevalent in our chromium carbide deposits. It also leads to increased roughness relative to nonconducting codeposits shown schematically in Figure 16b.

Particle surface charges and ζ potential play an important role in transport and codeposition.[14,15,17,18] Lack of gravitational forces could alter the number of electrolyte ions adsorbed onto the particle surface relative to that in 1*g*. Depending on the nature of the induced charges, a particle could be shielded from or attracted to the cathode. Large nonconducting diamond particles with smaller charge/size ratio exhibited enhanced codeposition, as opposed to submicron diamonds. This behavior seems to indicate negative ion adsorption on the particle surface, which shields it from the cathode. Conductive chromium carbide particles showed an opposite trend (although more subtle) where larger chromium carbide with smaller charge/size ratio code-

(15) Zahavi, J.; Hazan, J. *Plating Surf. Finishing* **1983**, *70*, No. 2, 57.
(16) Foster, J.; Cameron, B. *Trans. Inst. Met. Finishing* **1976**, *54*, 178.
(17) Zahavi, J. Kerbel, H. *Plating Surf. Finishing* **1982**, *69*, 76.
(18) Kariapper, A. M. J.; Foster, J. *Trans. Inst. Met. Finishing* **1974**, *52*, 87.

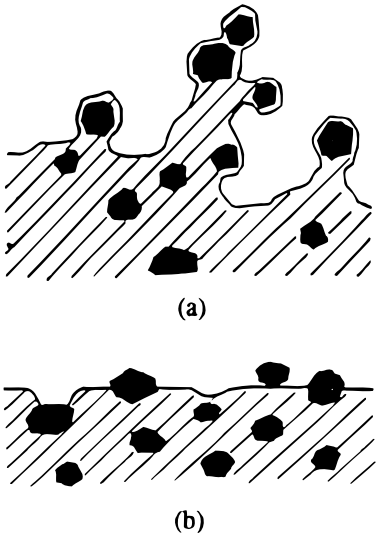

Figure 16. Schematic representation of a composite containing conducting particles (a) and nonconducting particles (b) and the influence on the surface.

posited in lower volume percent than smaller chromium carbide with larger charge/size ratio. This would indicate positive ions are adsorbed on the chromium carbide surface enhancing the attraction of the smaller particles to the cathode. Transport to the cathode could be impacted by the adsorbed ions which might cause increased drag. In a reduced-gravity environment, adsorption and drag could have different magnitudes. These factors could be the cause of the noted differences between particle volume percents of low-*g* and 1*g* samples. The implications of the above mentioned parameters on the deposition rate of particles has been described by Kariapper and Foster.[18]

5. Conclusions

Uniform surface distribution of particles in the metal matrix is more readily obtained under low-gravity environment. Particle sedimentation and edge effects are reduced regardless of the size, density, or nature of the particles.

Volume percent of codeposited nonconductive particles is greatly improved for large size particles in low *g* (45 μm). These particles are difficult to incorporate in the metal when making bench codepositions. Lack of gravitational force may cause different mechanisms of ionic adsorption on a particle's surface, and consequently different particle/particle and particle/cathode interactions. This factor along with the long adsorption time achievable in low *g* allowed the deposition of large diamond particles.

Volume percent of small nonconductive particles (<1 μm) is not enhanced by the low-*g* conditions in comparison to 1*g* experiments, while that of 5 μm particles produces similar results to the 1*g* controls.

There is evidence from KC-135 reduced gravity experiments of particle clumping when suspended in the electrolyte. Appropriate surfactants counteracted this behavior.[1] The clumping may be due to the success of weak attractive forces between the particles in the absence of stronger gravitational force.

Acknowledgment. The financial support of McDonnell Douglas corporation and NASA through the Center for Materials Development in Space at the University of Alabama in Huntsville is gratefully acknowledged. The authors thank H. Dwain Coble and McDonnell Douglas engineers for their technical assistance.

CM950483J